Human Molecular Genetics, 2023, Vol. 32, 3, 462–472
https://doi.org/10.1093/hmg/ddac210
Advance access publication date 24 August 2022
Original Article

YWHAZ variation causes intellectual disability and global developmental delay with brain malformation

Rui-Ping Wan[1], Zhi-Gang Liu[1], Xiao-Fei Huang[1], Ping Kwan[2], Ya-Ping Li[3], Xiao-Chong Qu[3], Xing-Guang Ye[1], Feng-Ying Chen[4], Da-Wei Zhang[4], Ming-Feng He[3], Jie Wang[3], Yu-Ling Mao[5,6] and Jing-Da Qiao[3,*]

[1]Department of Pediatrics, Affiliated Foshan Maternity & Child Healthcare Hospital, Southern Medical University, Foshan, Guangdong 528011, China
[2]School of Veterinary Science, University of Sydney, Sydney 2050, Australia
[3]Department of Neurology, Institute of Neuroscience, Key Laboratory of Neurogenetics and Channelopathies of Guangdong Province and the Ministry of Education of China, The Second Affiliated Hospital, Guangzhou Medical University, Guangzhou 510260, China
[4]Department of Radiology, Affiliated Foshan Maternity & Child Healthcare Hospital, Southern Medical University, Foshan, Guangdong 528011, China
[5]Department of Obstetrics and Gynecology, Center for Reproductive Medicine, Key Laboratory for Major Obstetric Diseases of Guangdong Province, The Third Affiliated Hospital of Guangzhou Medical University, Guangzhou 510150, China
[6]Key Laboratory for Reproductive Medicine of Guangdong Province, The Third Affiliated Hospital of Guangzhou Medical University, Guangzhou 510150, China
*To whom correspondence should be addressed at: Department of Neurology, Institute of Neuroscience, Key Laboratory of Neurogenetics and Channelopathies of Guangdong Province and the Ministry of Education of China, The Second Affiliated Hospital, Guangzhou Medical University, Guangzhou 510260, China.
Tel: 86-13242327861; Email: Joaquinqjd@163.com

Abstract

YWHAZ encodes an adapter protein 14–3-3ζ, which is involved in many signaling pathways that control cellular proliferation, migration and differentiation. It has not been definitely correlated to any phenotype in OMIM. To investigate the role of *YWHAZ* gene in intellectual disability and global developmental delay, we conducted whole-exon sequencing in all of the available members from a large three-generation family and we discovered that a novel variant of the *YWHAZ* gene was associated with intellectual disability and global developmental delay. This variant is a missense mutation of *YWHAZ*, p.Lys49Asn/c.147A > T, which was found in all affected members but not found in other unaffected members. We also conducted computational modeling and knockdown/knockin with *Drosophila* to confirm the role of the *YWHAZ* variant in intellectual disability. Computational modeling showed that the binding energy was increased in the mutated protein combining with the ligand indicating that the c147A > T variation was a loss-of-function variant. Cognitive defects and mushroom body morphological abnormalities were observed in *YWHAZ* c.147A > T knockin flies. The *YWHAZ* knockdown flies also manifested serious cognitive defects with hyperactivity behaviors, which is consistent with the clinical features. Our clinical and experimental results consistently suggested that *YWHAZ* was a novel intellectual disability pathogenic gene.

Received: May 16, 2022. **Revised:** August 2, 2022. **Accepted:** August 17, 2022

Graphical Abstract

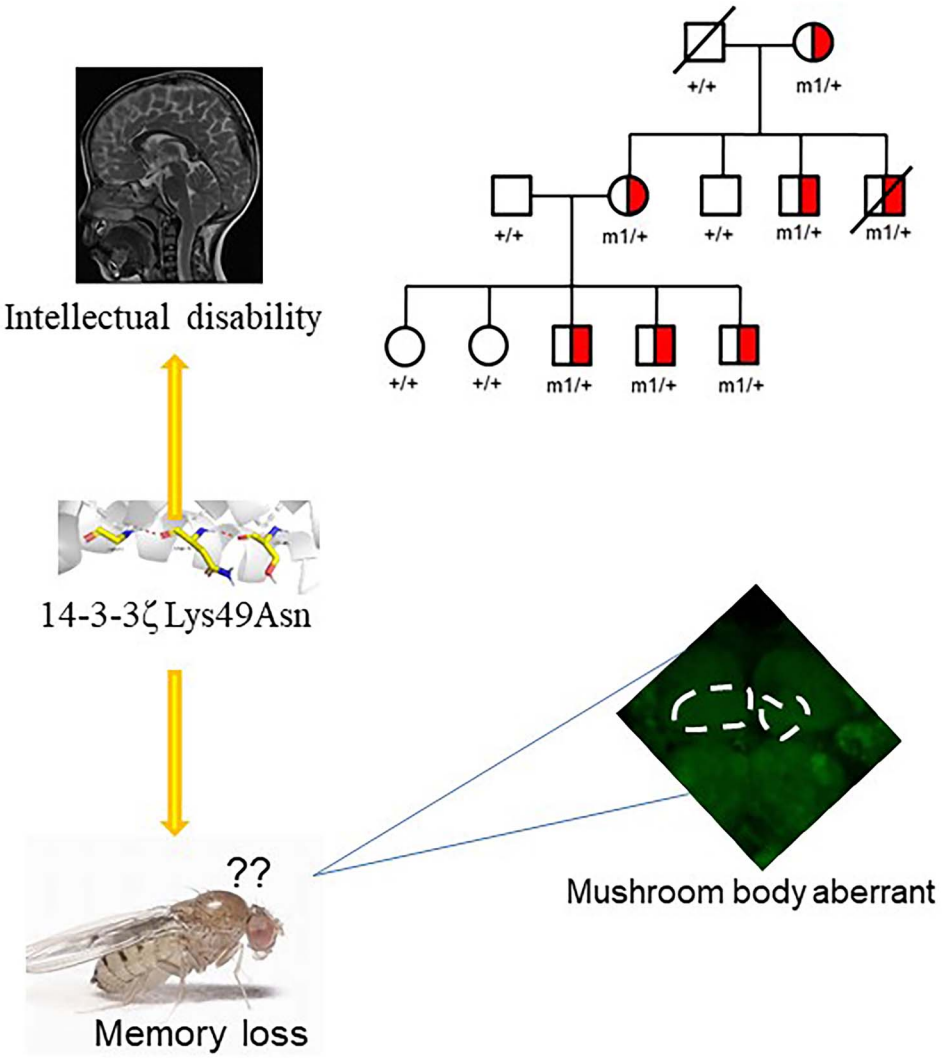

Introduction

Intellectual disability (ID) and global developmental delay (GDD) are common concerns in pediatric clinics. To this day, the prevalence of ID/GDD is about 1–3% of the general population (1). Etiologies of ID/GDD are highly complex, comprising extrinsic factors, such as acquired brain injury and intrinsic genetic factors (2,3). Up to one-half of the unexplained ID/GDD are estimated to be genetic origin, especially in the moderate or severe cases (4). As body physiology is functioning with complex molecular networks, the spatio-temporal expression of many proteins in the brain needs to be regulated accurately and delicately (5). Therefore, variations affecting any genes encoding these proteins can result in serious consequences for the brain structure and/or its function. With the recent advances in genetic technologies, next-generation sequencing, new ID/GDD genes can be identified rapidly. Until 2016, > 700 genes have been identified, including the X-linked, autosomal-dominant and autosomal-recessive genes (6). Despite these successes, the genetic background of a large number of patients with ID/GDD remains unknown.

YWHAZ (OMIM*601288) encodes tyrosine 3-monooxygenase/tryptophan 5-monooxygenase activation protein zeta (14–3-3ζ), one member of the 14–3-3 protein family which is highly conserved among different species. 14–3-3ζ is ubiquitously expressed in the brain and other tissues. It plays an important role in diverse signaling pathways to regulate cellular proliferation, migration and differentiation by binding to phosphoserine-containing proteins (7). Although the association of *YWHAZ* variants with schizophrenia and other neurodevelopmental disorders has been reported in recent years (8,9), the pathogenicity is not well studied yet.

In this study, we conducted a whole-exome sequencing for all members of a three-generation family in which there are seven patients with ID/GDD. A heterozygous variation in *YWHAZ* segregated with the disease phenotype was identified. Bioinformatic analysis, computational modeling and functional experiments with *Drosophila* knockin and knockdown models suggested that *YWHAZ* is a causative gene candidate of ID/GDD.

Results

Clinical findings

In this study, there were seven patients with ID/GDD from the same family but in three generations, involving both male and female members (Fig. 1). The main clinical features of the affected

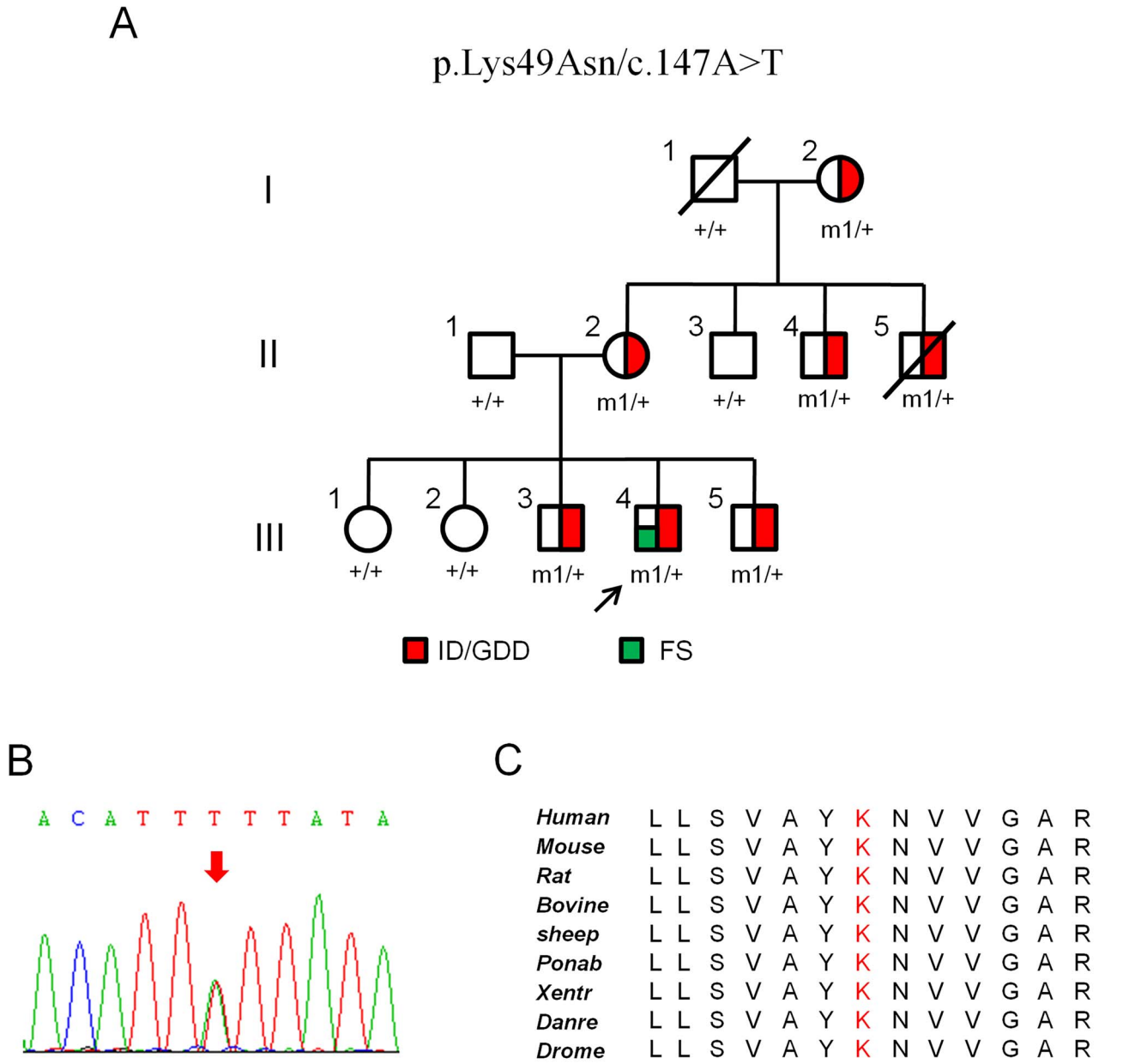

Figure 1. Genetic data of cases with *YWHAZ* variants. (**A**) Pedigrees of the family with *YWHAZ* variants and their corresponding phenotypes. (**B**) DNA sequencing chromatogram of the *YWHAZ* c.147A > T variants. (**C**) Amino acid sequence alignment of *YWHAZ* p.Lys49Asn variants showed that the Lys49 is highly conserved across species.

subjects are summarized in Table 1. The proband (III-4) was a boy admitted to the hospital diagnosed with GDD, febrile seizures and abnormal behavior including hyperactivity and head bumping. He was born at full term following normal spontaneous labor without any complications. He could speak <10 single words when he was a preschooler. The proband experienced two episodes of febrile seizures between 2 and 3 years old. Physical examinations did not reveal any specific positive signs, except for short stature and an isolated cafe-au-lait macule on the right inner thigh. Gesell developmental scale (GDS) total development quotient (DQ) was 37. Brain magnetic resonance imaging (MRI) showed simplified gyral pattern, smaller volume of posterior cranial fossa and decreased brainstem-tentorium angle (Fig. 2). Electroencephalogram (EEG) showed slightly faster background rhythms without epileptic discharges. No abnormality was found in biochemical and metabolic laboratory results. His two brothers (III-3 and III-5) also had GDD and hyperactivity with short stature. The elder brother was late walking and could speak only two-character words in middle childhood. Wechsler total IQ was <41. The early motor and speech developmental milestones of the younger brother were slightly delayed. GDS total DQ was 54 when he was a toddler. Their mother, two uncles and grandmother (II-2, II-4, II-5, I-2) had mild ID and were able to perform simple work. One of the uncles died in an accident in his 20s. The mother had abnormal behavior, such as mood fluctuation, irritability, self-giggle and self-talking (Supplementary Material, Table S1). Brain MRI of the two brothers and the mother displayed brain malformation as the proband (Fig. 2).

Table 1. Clinical features of the affected individuals

Patient	Gender	Age at assessment	Degree of ID/GDD	IQ/DQ test	Seizures	Behavior problems	Neurologic signs	Brain MRI	EEG
I-2	Female	60s	Mild	NA	No	No	No abnormalities	NA	NA
II-2	Female	40s	Mild	NA	No	Mood fluctuation, irritability, self-giggle, and self-talking	No abnormalities	Simplified gyral pattern, small volume of posterior cranial fossa and decreased brainstem-tentorium angle	NA
II-4	Male	30s	Mild	NA	No	No	No abnormalities	NA	NA
II-5	Male	Died in his 20s	Mild	NA	No	No	NA	NA	NA
III-3	Male	Middle childhood	Severe	WISC total IQ < 41	No	Hyperactivity	No abnormalities	Simplified gyral pattern, small volume of posterior cranial fossa and decreased brainstem-tentorium angle	Background EEG rhythms are slightly faster
III-4 (the proband)	Male	Toddler	Severe	GDS total DQ 37	FS between 2 and 3 years	Self-harming behavior (headbanging), hyperactivity	An isolated cafe-au-lait Macule	Simplified gyral pattern, small volume of posterior cranial fossa and decreased brainstem-tentorium angle	Background EEG rhythms are slightly faster
III-5	Male	Toddler	Mild to moderate	GDS total DQ 54	No	Hyperactivity	No abnormalities	Simplified gyral pattern, small volume of posterior cranial fossa, and decreased brainstem-tentorium angle	Normal

Abbreviations: EEG, electroencephalogram; FS, febrile seizures; GDS, Gesell developmental scale; ID/GDD, intellectual disability/global developmental delay; IQ/DQ, intelligence quotient/development quotient; MRI, magnetic resonance imaging; NA, no available; WISC, Wechsler intelligence scale for children.

Identification of *YWHAZ* variation

We conducted whole-exome sequencing on the proband (III-4), two affected brothers (III-3, III-5), one unaffected sister (III-1) and their parents (II-1, II-2). After family analysis of the variant data, 10 rare variants located in 10 genes (*ARHGAP4*, *AGPS*, *APOL3*, *CES3*, *DACT2*, *ECH1*, *FAM71E2*, *KREMEN1*, *YWHAZ*, *ZFYVE26*) that co-segregated with the ID/GDD phenotype were identified. Sanger sequencing was used to validate the candidate variations and the variants in other family members (III-2, II-3, II-4, I-2) were analyzed further for the segregation. We identified a heterozygous missense variation c.147A > T in *YWHAZ* in all available affected members of the family, whereas the unaffected members have no variation (Fig. 1). The variants in *ARHGAP4*, *AGPS*, *APOL3* and *KREMEN1* were not found in the affected uncle (II-4) and grandmother (I-2). The variants in *CES3*, *DACT2*, *ECH1*, *FAM71E2* and *ZFYVE26* were either detected in the unaffected sister (III-2) or uncle (II-3) (Supplementary Material, Table S2). Thus, the *YWHAZ* variation was considered as the pathogen in this family.

YWHAZ, encoding 14–3-3 ζ, is highly conserved in different species and abundantly expressed in the brain. Homozygous *Ywhaz* knockout mice display neurodevelopmental and neuropsychiatric behavioral defects (http://www.informatics.jax.org/marker/MGI:109484). The c.147A > T variation in *YWHAZ* led to a substitution of asparagine for lysine at codon 49 of the 14–3-3ζ protein (p.Lys49Asn), and was not present in any public databases, including the 1000 Genomes Project, ESP, ExAC and gnomAD (Table 2). Sequence alignments suggested that the mutation site was highly conserved in various species (Fig. 1). Moreover, most commonly used silico tools predicted that the missense variation is damaging (Table 2).

Ywhaz knockin in flies

ID and developmental delay are the major phenotypes in the family with *YWHAZ* variation. To confirm the effect of c.147A > T missense variation of *YWHAZ*, the c.147A > T missense variation knockin fly was created by using the CRISPR/Cas9 system. The DNA sequence of the knockin fly was confirmed by Sanger sequencing (Fig. 3A). In the short-term aversive olfactory memory test, the c.147A > T knockin flies showed significant memory defect, lower PI, compared with the wild-type flies (0.11 ± 0.04, $n = 5$ vs. 0.46 ± 0.06, $n = 5$, $^{**}P = 0.002$, Fig. 3B). The odor avoidance test and shock avoidance test were used to exclude the basic disturbance of odor and shock performances in different genotypes of flies (Fig. 3C and D).

Febrile seizures were also observed in the proband, thus we used mechanical stimulus to test seizure-like behavior in c.147A > T knockin flies. No obvious seizure behavior was observed in c.147A > T knockin flies (Fig. 3E). This suggested that febrile seizures were not relative to the c.147A > T variation.

Brain structure in *Ywhaz* knockin flies

The II-2, III-3, III-4 and III-5 members exhibited abnormal brain structure in MRI, thus we further studied the brain morphology in knockin flies. The mushroom body is an important brain structure in flies for cognitive functions such as learning and memory (10). There are three major substructures in the mushroom body:

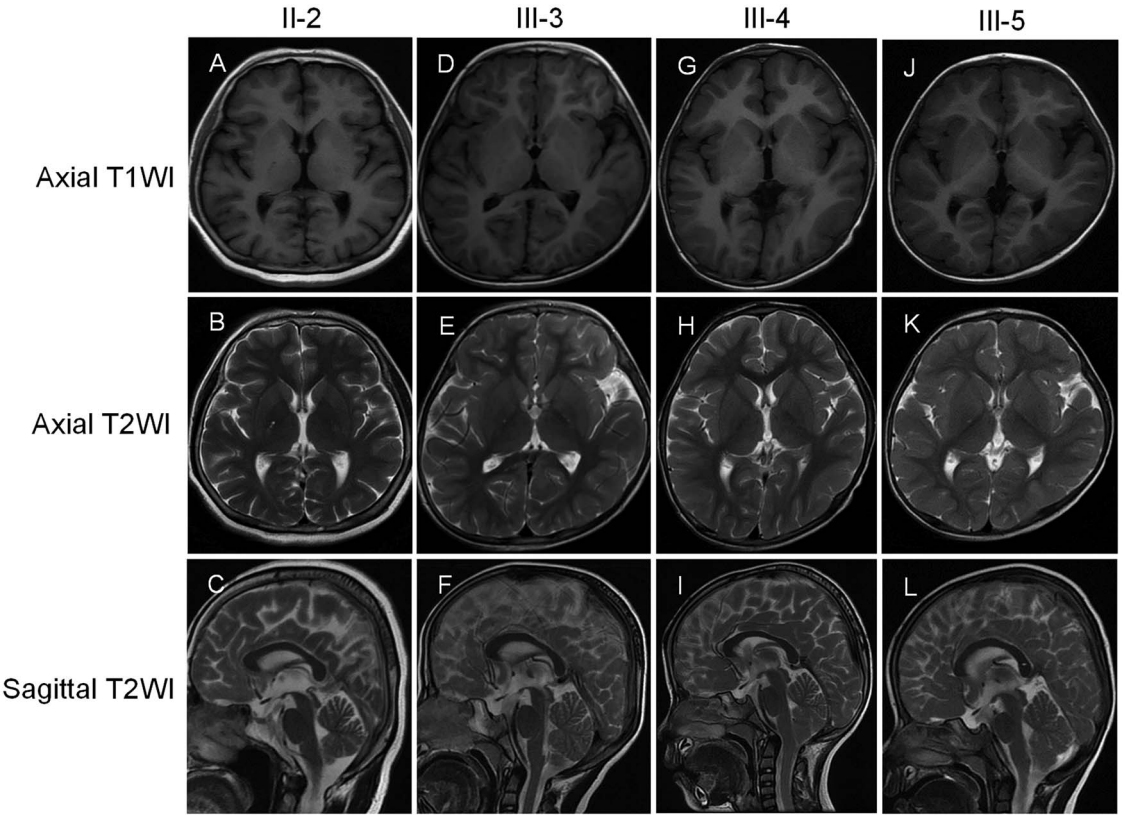

Figure 2. Brain MRI in subjects with *YWHAZ* variation axial (the above two rows) and mid-sagittal (the third row) images are shown from subjects II-2 (**A–C**), III-3 (**D–F**), III-4 (**G–I**), and III-5 (**J–L**). Images of the cortex reveal different degrees of diffuse simplified gyral pattern, with slightly shallow sulci and a reduced number of gyri. Generally, the width of the gyri is equal to the depth of the sulci. The mid-sagittal images demonstrate small volume of posterior cranial fossa, and decreased brainstem-tentorium angle (<30 degrees).

Table 2. Genetic characteristics of the *YHWAZ* variation

Gene	Nucleotide change	Amino acid change	MAF				SIFT	Polyphen2_HVAR	Mutation taster	CADD	LRT
			KG	ESP	ExAC	gnomAD					
YWHAZ	c.147A > T	p.Lys49Asn	NA	NA	NA	NA	T (0.059)	D (0.999)	D (1.000)	D (25.1)	D (0.000)

CADD, combined annotation dependent depletion; D, damage/deleterious; ESP, NHLBI Exome Sequencing Project; ExAC, Exome Aggregation Consortium; gnomAD, Genome Aggregation Database; KG, the 1000 Genomes Project; LRT, a likelihood ratio test; MAF, minor allele frequency; NA, not available; T, tolerable.
GenBank accession number for *YWHAZ*: NM_001135699

alpha/beta lobes, alpha′/beta′ lobes and gamma lobes. Different substructures of mushroom body were responsible for different time-phases of memory (11,12). Under the Green Fluorescent Proteins (GFP) guiding, mushroom body lobes can be identified clearly. The gamma lobes of knockin flies were smaller than that of wild-type flies ($3420 \pm 163.2\ \mu m^2$, $n = 3$ vs. $4303 \pm 88.2\ \mu m^2$, $n = 3$, $^{**}P = 0.0089$, Fig. 4A, B and E). The alpha/beta lobes and alpha′/beta′ lobes showed no difference between wild-type flies and knockin flies (Fig. 4C and D).

3D modeling and docking

The 14–3-3ζ p.Lys49Asn (c.147A > T) variant protein was successfully modeled by the SWISS-MODEL. Variant Asn49 formed fewer hydrogen bonds between adjacent amino acids than that of wild-type Lys49 (2 vs. 5. Fig. 5A and B), suggesting 14–3-3 p.Lys49Asn may disturb hydrogen bonds and structural stability. Phosphopeptide is an important ligand of 14–3-3ζ (13), and protein–protein docking results showed that Lys49Asn/c.147A > T potentially altered the docking energy in the phosphopeptide-14-3-3ζ complex, with a significant increase of Gibbs free energy (from −6.13 kcal/mol to −4.16 kcal/mol. Figure 5C–F). This indicated that Lys49Asn/c.147A > T could decrease the binding ability to phosphopeptide, which suggested Lys49Asn/c.147A > T would be a loss-of-function variation.

Ywhaz loss of function in flies

The computational protein modeling results suggested that Lys49Asn/c.147A > T would be a loss-of-function variation. Thus, we established *Ywhaz* knockdown flies, *tub > 14–3-3ζ-RNAi*, to further study the 14–3-3 function. In the memory test, we found that *Ywhaz* knockdown flies also showed lower memory index than that of the wild-type flies (0.17 ± 0.02, $n = 5$ vs. 0.55 ± 0.04, $n = 5$, $^{****}P < 0.0001$, Fig. 6A), which is consistent to our previous results (Fig. 3B). The knockdown efficiency of *tub > 14–3-3ζ-RNAi* flies was about 50.5% (Fig. 6B). The *Ywhaz* knockdown flies also showed no seizure-like behavior (Fig. 6C) as the c.147A > T knockin flies. Interestingly, about 70% of the *Ywhaz* knockdown flies showed hyperactivity-like behaviors with repetitive non-flying wing

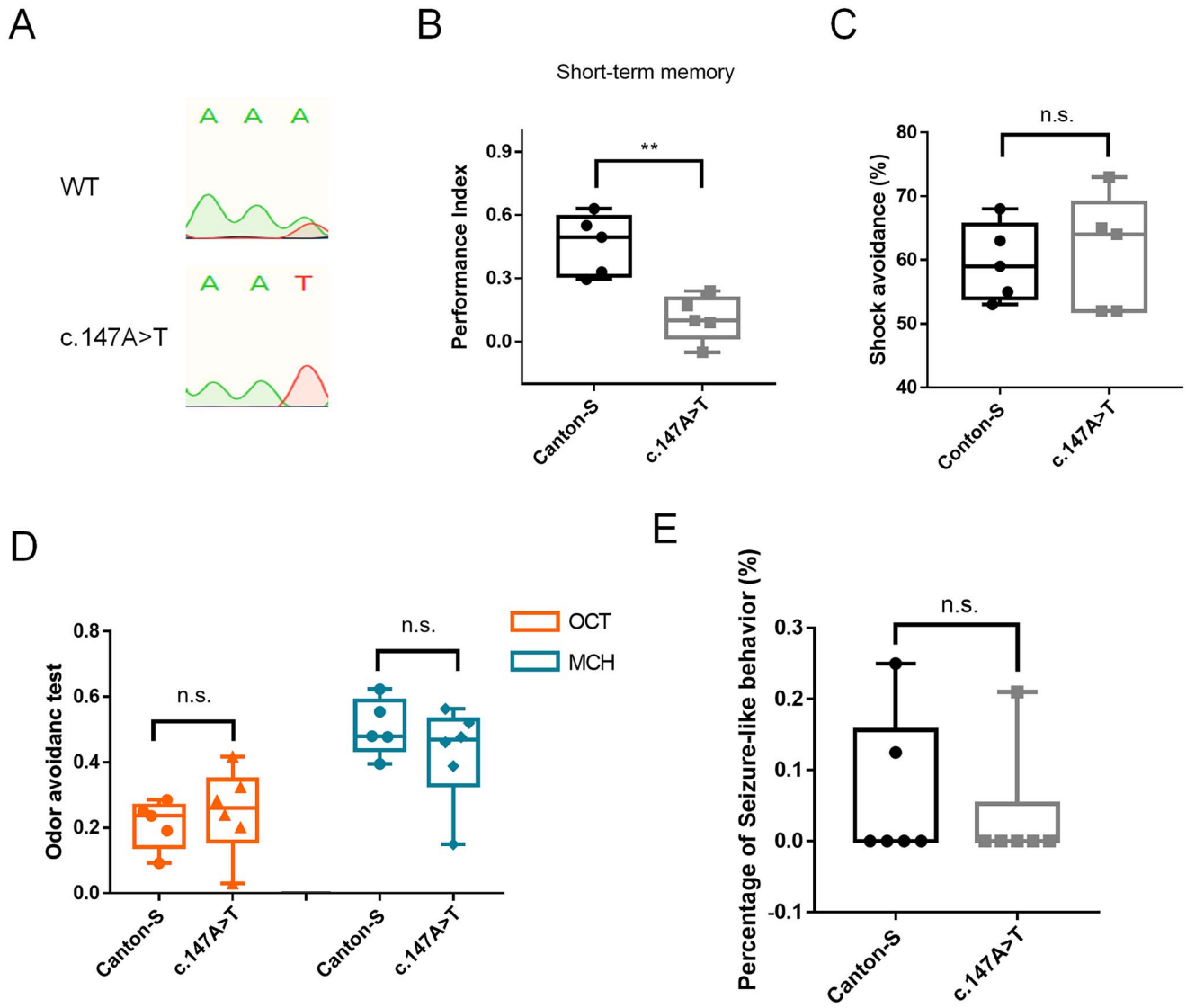

Figure 3. Behavior performance of *YWHAZ* knockin flies. (**A**) DNA sequencing of the knockin fly and wild-type fly. (**B**) Short-term memory performance of *YWHAZ* knockin flies. (**C**) Electrical shock test of knockin and wild-type flies. (**D**) Odor avoidance test of knockin and wild-type flies. (**E**) Bang-sensitive test of knockin and wild-type flies.

vibration (Fig. 6D) and repetitive drop and jump (Fig. 6E), and this hyperactivity behavior was not observed in the wild-type flies (Fig. 6F). In clinical data, three members (III-3, III-4, III-5. Table 1) have hyperactivity features. This feature can be also caused by 14–3-3 dysfunction. To further confirm that the c.147A > T is loss-of-function variant, we cross *Ywhaz* knockdown flies with c.147A > T knockin flies to establish *tub/c.147A > T; 14–3-3zeta-RNAi* flies. The cognitive performance of *tub/c.147A > T; 14–3-3zeta-RNAi* flies showed no difference with that of *Ywhaz* knockdown flies (0.15 ± 0.02 vs. 0.17 ± 0.03, $n = 6$, $P = 0.60$), suggesting that c.147A > T is not gain-of-function variant (Fig. 6G).

Discussion

We clarified a novel pathogenic variant, *YWHAZ* c.147 T > A, from a large three-generation family with ID. The *YWHAZ* encoded tyrosine 3-monooxygenase/tryptophan 5-monooxygenase activation protein ζ that is intolerant to both LoF (pLI = 0.94) and missense (Z = 3.1) variant on the basis of the gnomAD (v2.2.1). *YWHAZ* was involved in multifunction in various tissues and organs. It could promote epithelial–mesenchymal transition by elevated ERK1/2 phosphorylation in hepatocellular carcinoma and inhibit Cdc2 phosphorylation in lung cancer cells (14). In the mouse study, knockout of *YWHAZ* could improve glucose tolerance by elevating glucagon-like peptide-1 (GLP-1) synthesis and increasing GLP-1 release (15). The neurodevelopmental defect was also observed in the *YWHAZ*-deficient mice (16).

In this study, we identified the *YWHAZ* Lys49Asn variant in seven members of a large three-generation family with total 12 members. All these seven members with Lys49Asn had either mild or severe ID/GDD. All the third-generation members had low IQ/DQ, motor development delay, speech development delay and hyperactivity behavior. Thus, the *YWHAZ* Lys49Asn variant may affect neurodevelopment and cognitive functions. Our *YWHAZ* Lys49Asn knockin flies showed a low cognitive performance index (PI) (Fig. 3) and aberrant mushroom body structure (Fig. 4). The mushroom body is a crucial structure for fly cognitive function. The experimental results and clinical data consistently suggested that *YWHAZ* would be an ID/GDD pathogenic gene. Febrile seizure was not found in our case except the proband (Fig. 1A), and the

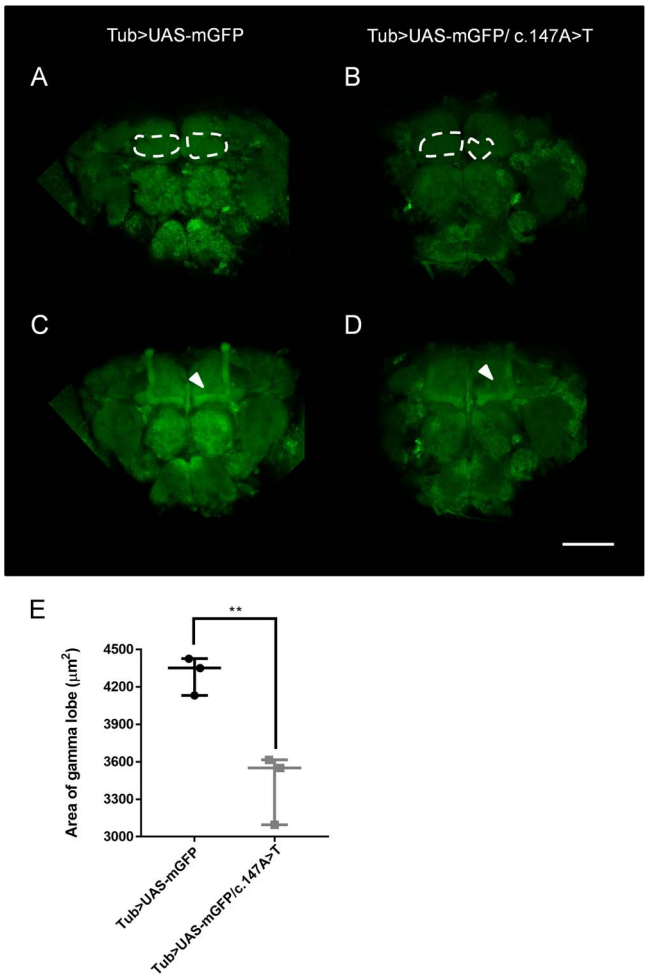

Figure 4. Brain morphology of *YWHAZ* knockin flies. (**A**) Wild-type and (**B**) *YWHAZ* knockin fly brain structure: dotted line indicated the gamma lobes of the mushroom body. (**C**, **D**) Alpha/beta lobes and alpha′/beta′ lobes of wild-type (C) and knockin flies (D). Scale bar: 100 μm. (E) Average area of gamma lobes in wild-type and *Ywhaz* knockin flies.

fly behavior test also showed no classical seizure-like behavior (Fig. 3E). This indicated that febrile seizure or epilepsy should not be a common feature in this large three-generation family with the *YWHAZ* variation. However, it cannot entirely exclude the possibility that seizure or epilepsy is a subsequent outcome form of *YWHAZ* variation and the hyperactivity behavior is a non-classical seizure-like behavior in the *Ywhaz* knockdown flies.

YWHAZ variation has not been correlated to any phenotype in OMIM. Ivan K. Popov *et al.* had reported that *YWHAZ* Ser230Trp variant is a gain-of-function variation in the RAS–ERK pathway, which was associated with Cardiofaciocutaneous syndrome; however, the patient also carried *SCN8A* variant in that case (9). In our results, 10 rare variants were found in this large family (*ARHGAP4*, *AGPS*, *APOL3*, *CES3*, *DACT2*, *ECH1*, *FAM71E2*, *KREMEN1*, *YWHAZ*, *ZFYVE26*) but only *YWHAZ* variant perfectly match the phenotypes of all affected and unaffected members in that family. In addition, *YWHAZ* knockin flies showed relative behavioral and morphological phenotypes with the clinical case. The computational modeling (Fig. 5) and knockdown crossed with knockin animal results (Fig. 6G) further suggested that the *YWHAZ* Lys49Asn variant should be a loss-of-function variant.

Interestingly, the II-2 (irritability), III-3 (hyperactivity), III-4 (hyperactivity) and III-5 (hyperactivity) members exhibited irritability/hyperactivity behavior besides ID/GDD (Table 1), and these four members also carried variants of another four genes: *ARHGAP4*, *AGPS*, *APOL3*, *KREMEN1*(Supplementary Material, Table S2). This suggested that these four genes may be directly associated with irritability/hyperactivity phenotype, or may interact with *YWHAZ* to promote irritability/hyperactivity phenotype. Furthermore, III-3 (male), III-4 (male) and III-5 (male) but not II-2 (female) also showed severer degree of ID/GDD than other family members (Table 1). As the *ARHGAP4* is a gene on the X chromosome, it may interact with *YWHAZ* and induce severer ID/GDD in this family. Actually, hyperactivity and lower cognitive index were also observed in the *YWHAZ* knockdown flies but not in knockin flies (Figs 3 and 6). The clinical and experimental data consistently suggested that hyperactivity and severe ID/GDD occurred simultaneously in the *YWHAZ*-associated disorder. And the effect of *YWHAZ* variants with *ARHGAP4* variants in our case would be equivalent to the effect of *YWHAZ* knockdown. However, the interaction between *ARHGAP4* between *YWHAZ* should be further studied.

In summary, we identified the *YWHAZ* Lys49Asn variant in a three-generation family with ID/GDD. By combining the results from the whole-exon sequencing analysis, computational modeling test, knockin animal cognitive function and morphological tests, and knockdown animal behavior tests, we suggested that *YWHAZ* would be a novel ID/GDD pathogenic gene. *YWHAZ* function-related drugs or *YWHAZ* nanoliposomes could be considered applied to the *YWHAZ* variant patients, and this would be a potential therapeutic strategy for precision medicine.

Materials and Methods

Patients

Members in which there are seven patients from a large three-generation family were recruited from the Children Rehabilitation Center of Foshan Women and Children Hospital affiliated to the Southern Medical University. Clinical data were collected, including gender, age, perinatal history, neurodevelopmental history, family history, and general and neurological examinations. Wechsler intelligence scale for children (WISC) and GDS were used to evaluate intelligence quotient (IQ) or DQ. Brain MRI was conducted to detect brain structure abnormalities. EEG was performed to monitor abnormal rhythms and discharges. ID was defined as a disability characterized by significant limitations both in intellectual functioning and in adaptive behavior as expressed in conceptual, social and practical adaptive skills, which originated before 18 years of age (17). GDD was defined as a significant delay in two or more developmental domains, including gross or fine motor, speech/language, cognitive, social/personal and activities of daily living, and is being considered as a diagnostic criterion of ID (18). This study was approved by the ethics committee of the hospital. Signed informed consents were obtained from the participants or their parents. This study was approved by the ethics committee of Affiliated Foshan Maternity & Child.

Healthcare Hospital and Southern Medical University (No. FSFY-MEC-2018–016) had received written informed patient consent in this study.

Whole-exome sequencing and analysis

Blood samples were obtained from the proband, his siblings, their parents and other available family members. Qiagen Flexi

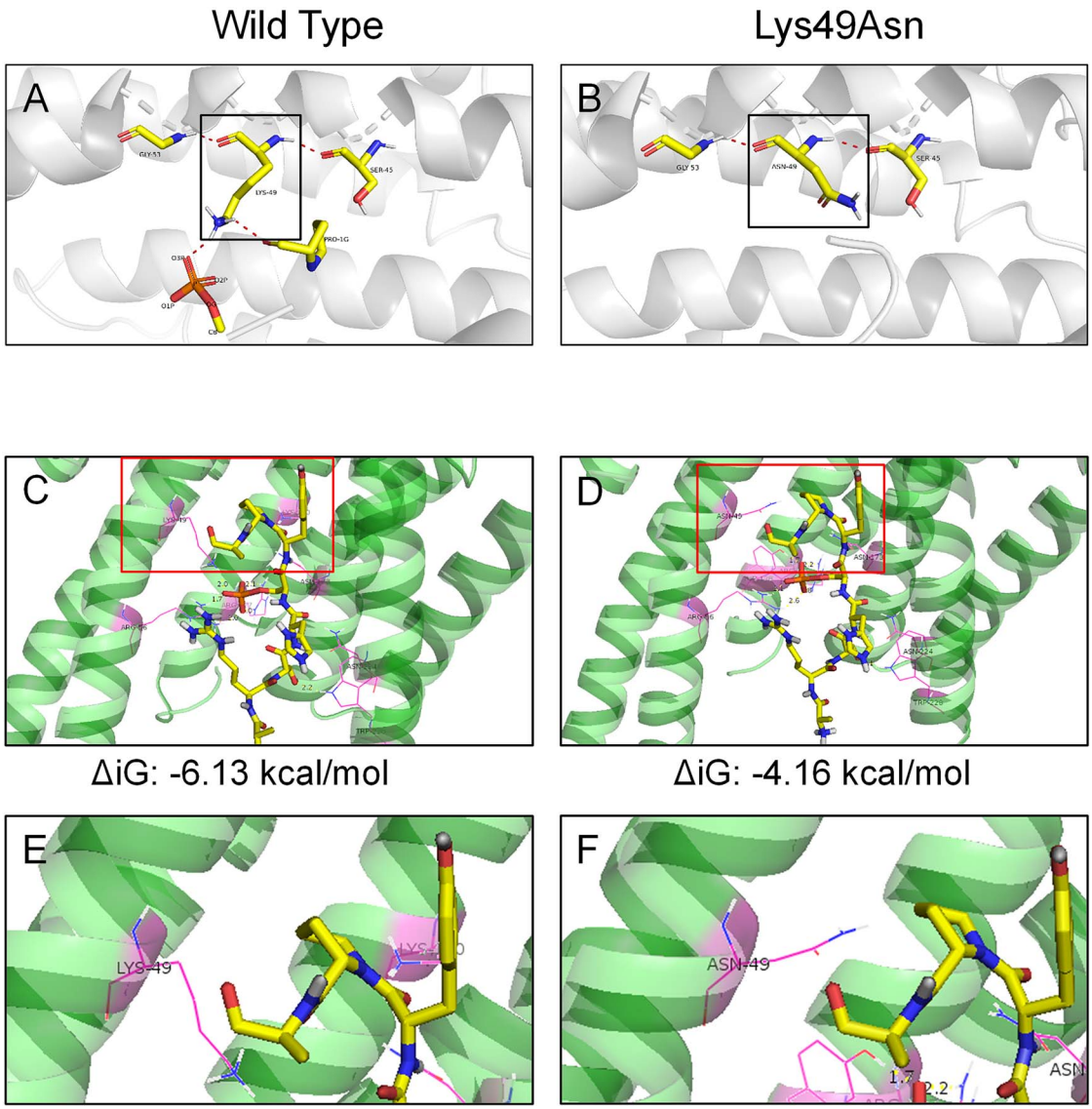

Figure 5. 3D protein model of 14–3-3 Lys49Asn variants. (**A**, **B**) Schematic illustration of hydrogen bonds in wild-type 14–3-3ζ (A) and Lys49Asn variants (B). The black rectangle indicated the 49 amino acids in 14–3-3ζ. (**C**, **D**) Model of calmodulin docking on 14–3-3ζ and the Lys49Asn variants.

Gene DNA kit (Qiagen, Hilden, Germany) was used to extract genomic DNA from peripheral blood. Whole-exome sequencing was carried out on an Illumina HiSeq 2000 instrument in accordance with standard procedures as previously described (14,19). Public databases including 1000 Genomes Project, NHLBI Exome Sequencing Project (ESP), Exome Aggregation Consortium (ExAC) and Genome Aggregation Database (gnomAD) were used to filter variants with a minor allele frequency (MAF) ≥ 0.005. We recruited 296 healthy volunteers as normal controls. Variant sites with a read depth below 10× were excluded as the low-quality data. Genes known to be associated with a non-neurological disease were also excluded. Further filtration for potentially pathogenic variants was on the basis of the family history and possible inheritance models. The candidate variants were validated by Sanger sequencing.

Bioinformatic analysis

Sequence alignments of multiple species were conducted to evaluate the evolutionary conservation of the variant. Software for functional prediction, including SIFT, PolyPhen-2, Mutation Taster, CADD and LRT, were used to predict the potential deleterious effect of the variant on protein function.

3D structural modeling and docking

3D structure of 14–3-3ζ modeling was carried out to predict the effect of the variant on protein structure by SWISS-MODEL (https://swissmodel.expasy.org/). The full-length structural model of 14–3-3ζ 1qjb.1.pdb was used as a template from the Protein Data Bank (PDB) (https://www.rcsb.org/). The protein structure was displayed by the PyMol Molecular Graphics System version 2.3. Phosphopeptide (PHOSPHOPEPTIDE 1qjb.1.pdb) was used as the ligand of 14–3-3ζ to predict the effect of the variant on protein function by AutoDock version 4.2.6.

Drosophila knockin and knockdown model

The establishment of the c.147A > T point mutation knockin model of *Ywhaz* in *Drosophila* was conducted by Qidong Fungene Biotechnology Co., Ltd (http://www.fungene.tech, China). In brief, w^{1118} was used as the background fly. Preparation of gRNA, preparation of cas9 mRNA, construction of donor plasmid,

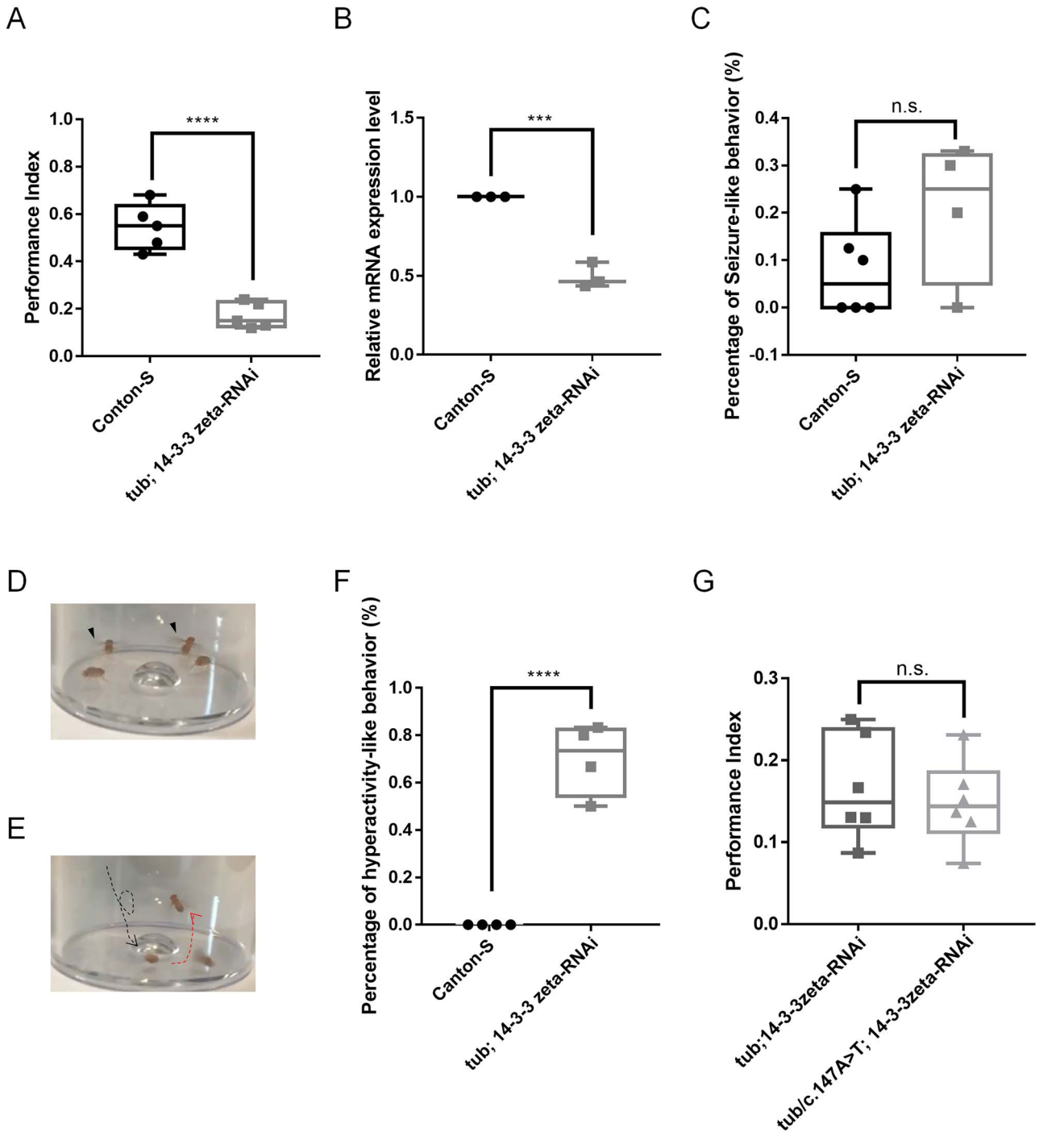

Figure 6. Behavior features of *YWHAZ* knockdown flies. (**A**) Short-term memory performance in *YWHAZ* knockdown flies. (**B**) Relative expression of mRNA in *YWHAZ* knockdown flies and wild-type flies. (**C**) Both *YWHAZ* knockdown flies and wild-type flies showed no classical seizure behavior in the Bang-sensitive test. (**D**, **E**) Hyperactivity-like behavior in Bang-sensitive test: repeat non-flying wing vibration (C) and repeat drop and jump (D). Black arrows indicated the wing vibration. Dotted lines showed the drop and jump trajectory. (**F**) About 70% of *YWHAZ* knockdown Flies showed hyperactivity-like behavior in the Bang-sensitive test. (**G**) *Ywhaz* knockdown flies and *Ywhaz* knockdown plus knockin flies show no significant difference in cognitive performance.

embryo injection, validation and balancing were performed in sequence. The gRNA sequences were: 17870-pm-sg1: GAAATGTGGTCGGTGCCCGC, 17870-pm-sg2: GTCCGTTGCCTACAAAAATG. Primer pair: 17870-pm-1F: atcactaatggaacattttctatgc, 17 870-pm-3R: AACGGATGGGATGTGTTGGCTG. The genotype of knockin fly is w[1118]; CG17870-RA-K52N/CyO. The sequencing result of the knockin fly was available online if necessary.

Ywhaz knockdown flies were crossed from *tub-Gal4* and *UAS-14-3-3ζ-RNAi* (CG17870, Bloomington Fly Stock Center, UAS). The knockdown efficiency of RNAi lines was checked by qPCR (*Taq* Pro Universal SYBR qPCR Master Mix, Vazyme, UK). The primer sequences are: F: ACACCGTTGTCGATGACTCG, R: ATCGAACGCCTGTTTAGCCA.

Behavior tests

Memory test

Aversive olfactory memory test was conducted by using T-maze equipment as previously mentioned (20). OCT (3-octanol, 0.1%

dilution in mineral oil) and MCH (4-methylcyclohexanol, 0.15% dilution in mineral oil) were used for odor stimulus. Twelve trains of 1.25-s pulses of 90 V with 3.75-s intervals were conducted as the electrical stimulus. At the training stage, one odor stimulus (conditioned stimulus, CS+) was paired with an electric shock (unconditioned stimulus, US+) for 60 s followed by a counter odor (CS−) without an electric shock for another 60 s with 30-s intervals. Then the trained flies were tested for 2 min with the exposure to the two odors simultaneously. Memory PI was calculated using the following formula: (CS− flies−CS+ flies)/(CS− flies + CS+ flies).

Odor test and electrical shock tests were used to evaluate the basic performance of different genotypes of flies. For the odor test, about 50 naive flies were exposed to one odor (OCT or MCH) and air at the same time. The PI was calculated as the percentage of flies that approached to the odor minus the percentage of flies that approached to air. For the electrical shock test, about 50 naïve flies were placed at the center between the two tubes with electrifiable grids. One of the electrifiable grid tubes were applied electrical stimulus for 2 min. The PI was calculated as the percentage of flies that avoided the electrical shock (positive) minus the percentage of flies that approach the electrical shock (negative).

Mechanical stimulation test

Mechanical stimulation test conducted on flies 3–5 days after eclosion to observe seizure-like behavior following the previous study with minor modulation. Flies were anesthetized with CO_2 and transferred to a new vial to recover for 1 day. About three to seven flies were placed in one vial and stimulated mechanically by a vortex mixer (VWR, USA) at maximum speed for 20 s. The percentage and duration of abnormal behavior in flies were acquired (21).

Morphology

The brain was dissected (22,23) and fixed with 4% paraformaldehyde in PBST for 1 h at room temperature, then washed and permeabilized three times with 0.3% PBST. Brain samples were mounted with mounting solution (Abcam). Morphological images were captured using a confocal microscope (SP8; Zeiss) and analyzed with ImageJ software. UAS-mGFP flies were used as a tool which cells' membranes were labeled with GFP.

Statistical analysis

All quantitative data are presented as mean ± SEM. The Student's *t*-test was used to compare two independent or paired samples. Statistical analyses were performed with GraphPad Prism 7.00 and SPSS 20. The cutoff value for statistical significance is $P < 0.05$.

Supplementary Material

Supplementary Material is available at *HMG* online.

Acknowledgements

Thanks Prof. Wei-Ping LIAO (the Second Affiliated Hospital of Guangzhou Medical University) for helping analyze the clinical data. Thanks for Dr Yan-Chao WANG (Qidong Fungene Biotechnology Co., Ltd) for helping establish knockin fly model.

Conflict of Interest statement. None declared.

Funding

Guangdong Basic and Applied Basic Research Foundation (No. 2020A1515110095 to R-P.W), the Second Affiliated Hospital of Guangzhou Medical University (to J-D.Q. Funding No. 2021004) and Guangzhou Postdoc Startup Fund (to J-D.Q).

Author Contributions

Jing-Da Qiao, Rui-Ping Wan, Yu-Ling Mao and Ping Kwan designed this study. Rui-Ping Wan, Zhi-Gang Liu, Xiao-Fei Huang, Xing-Guang Ye, Feng-Ying Chen, Da-Wei Zhang and Jie Wang collected and analyzed the clinical data. Ya-Ping Li and Ming-Feng He performed the computational modeling experiments. Jing-Da Qiao and Xiao-Chong Qu performed animal experiments. Jing-Da Qiao, Rui-Ping Wan and Ping Kwan wrote the manuscript.

References

1. Belanger, S.A. and Caron, J. (2018) Evaluation of the child with global developmental delay and intellectual disability. *Paediatr. Child Health*, **23**, 403–419.
2. Rauch, A., Wieczorek, D., Graf, E., Wieland, T., Endele, S., Schwarzmayr, T., Albrecht, B., Bartholdi, D., Beygo, J., Di Donato, N. *et al.* (2012) Range of genetic mutations associated with severe non-syndromic sporadic intellectual disability: an exome sequencing study. *Lancet*, **380**, 1674–1682.
3. Hamdan, F.F., Srour, M., Capo-Chichi, J.M., Daoud, H., Nassif, C., Patry, L., Massicotte, C., Ambalavanan, A., Spiegelman, D., Diallo, O. *et al.* (2014) De novo mutations in moderate or severe intellectual disability. *PLoS Genet.*, **10**, e1004772.
4. Obsil, T. and Obsilova, V. (2011) Structural basis of 14-3-3 protein functions. *Semin. Cell Dev. Biol.*, **22**, 663–672.
5. Li, F.Q., Mofunanya, A., Harris, K. and Takemaru, K. (2008) Chibby cooperates with 14-3-3 to regulate beta-catenin subcellular distribution and signaling activity. *J. Cell Biol.*, **181**, 1141–1154.
6. Vissers, L.E., Gilissen, C. and Veltman, J.A. (2016) Genetic studies in intellectual disability and related disorders. *Nat. Rev. Genet.*, **17**, 9–18.
7. Aghazadeh, Y. and Papadopoulos, V. (2016) The role of the 14-3-3 protein family in health, disease, and drug development. *Drug Discov. Today*, **21**, 278–287.
8. Fromer, M., Pocklington, A.J., Kavanagh, D.H., Williams, H.J., Dwyer, S., Gormley, P., Georgieva, L., Rees, E., Palta, P., Ruderfer, D.M. *et al.* (2014) De novo mutations in schizophrenia implicate synaptic networks. *Nature*, **506**, 179–184.
9. Popov, I.K., Hiatt, S.M., Whalen, S., Keren, B., Ruivenkamp, C., van Haeringen, A., Chen, M.J., Cooper, G.M., Korf, B.R. and Chang, C. (2019) A YWHAZ variant associated with Cardiofaciocutaneous syndrome activates the RAF-ERK pathway. *Front. Physiol.*, **10**, 388.
10. Akalal, D.B., Wilson, C.F., Zong, L., Tanaka, N.K., Ito, K. and Davis, R.L. (2006) Roles for drosophila mushroom body neurons in olfactory learning and memory. *Learn. Mem.*, **13**, 659–668.
11. Wang, Y.L., Mamiya, A., Chiang, A.S. and Zhong, Y. (2008) Imaging of an early memory trace in the drosophila mushroom body. *J. Neurosci.*, **28**, 4368–4376.
12. Akalal, D.B.G., Yu, D.H. and Davis, R.L. (2010) A late-phase, long-term memory trace forms in the gamma neurons of drosophila mushroom bodies after olfactory classical conditioning. *J. Neurosci.*, **30**, 16699–16708.

13. Kasinski, A., Dong, X., Khuri, F.R., Boss, J. and Fu, H. (2014) Transcriptional regulation of YWHAZ, the gene encoding 14-3-3zeta. *PLoS One*, **9**, e93480.
14. Gan, Y., Ye, F. and He, X.X. (2020) The role of YWHAZ in cancer: a maze of opportunities and challenges. *J. Cancer*, **11**, 2252–2264.
15. Lim, G.E., Piske, M., Lulo, J.E., Ramshaw, H.S., Lopez, A.F. and Johnson, J.D. (2016) Ywhaz/14-3-3zeta deletion improves glucose tolerance through a GLP-1-dependent mechanism. *Endocrinology*, **157**, 2649–2659.
16. Cheah, P.S., Ramshaw, H.S., Thomas, P.Q., Toyo-Oka, K., Xu, X., Martin, S., Coyle, P., Guthridge, M.A., Stomski, F., van den Buuse, M. *et al.* (2012) Neurodevelopmental and neuropsychiatric behaviour defects arise from 14-3-3zeta deficiency. *Mol. Psychiatry*, **17**, 451–466.
17. Musante, L. and Ropers, H.H. (2014) Genetics of recessive cognitive disorders. *Trends Genet.*, **30**, 32–39.
18. Toyo-oka, K., Wachi, T., Hunt, R.F., Baraban, S.C., Taya, S., Ramshaw, H., Kaibuchi, K., Schwarz, Q.P., Lopez, A.F. and Wynshaw-Boris, A. (2014) 14-3-3epsilon and zeta regulate neurogenesis and differentiation of neuronal progenitor cells in the developing brain. *J. Neurosci.*, **34**, 12168–12181.
19. Zhang, L., Jing, H., Li, H., Chen, W., Luo, B., Zhang, H., Dong, Z., Li, L., Su, H., Xiong, W.C. *et al.* (2020) Neddylation is critical to cortical development by regulating Wnt/beta-catenin signaling. *Proc. Natl. Acad. Sci. U. S. A.*, **117**, 26448–26459.
20. Pascual, A. and Preat, T. (2001) Localization of long-term memory within the drosophila mushroom body. *Science*, **294**, 1115–1117.
21. Wang, J., Qiao, J.D., Liu, X.R., Liu, D.T., Chen, Y.H., Wu, Y., Sun, Y., Yu, J., Ren, R.N., Mei, Z. *et al.* (2021) UNC13B variants associated with partial epilepsy with favourable outcome. *Brain*, **144**, 3050–3060.
22. Gu, H.Y. and O'Dowd, D.K. (2006) Cholinergic synaptic transmission in adult drosophila Kenyon cells in situ. *J. Neurosci.*, **26**, 265–272.
23. Qiao, J.D. and Mao, Y.L. (2020) Knockout of PINK1 altered the neural connectivity of drosophila dopamine PPM3 neurons at input and output sites. *Invertebr. Neurosci.*, **20**, 11.